IN-34
27030
28 P.

NASA Technical Memorandum 106737
ICOMP-94-22

Boundary Conditions for Unsteady Compressible Flows

S.I. Hariharan
Institute for Computational Mechanics in Propulsion
Lewis Research Center
Cleveland, Ohio

and The University of Akron
Akron, Ohio

and

D.K. Johnson
The University of Akron
Akron, Ohio

September 1994

National Aeronautics and
Space Administration

BOUNDARY CONDITIONS FOR UNSTEADY COMPRESSIBLE FLOWS

S.I. Hariharan*
Institute for Computational Mechanics in Propulsion
Lewis Research Center
Cleveland, Ohio 44135

and The University of Akron
Department of Mathematical Sciences
Akron, Ohio 44325

D.K. Johnson
The University of Akron
Department of Mathematical Sciences
Akron, Ohio 44325

Abstract

This paper explores solutions to the spherically symmetric Euler equations. Motivated by the work of Hagstrom and Hariharan [7] and Geer and Pope [5], we model the effect of a pulsating sphere in a compressible media. The literature available on this suggests that an accurate numerical solution requires artificial boundary conditions which simulate the propagation of nonlinear waves in open domains. Until recently, the boundary conditions available are in general linear, and based on non-reflection. Exceptions to this are the nonlinear non-reflective conditions of Thompson [11], and the nonlinear reflective condition of [7]. The former is based on the rate of change of the incoming characteristics, while the latter relies on asymptotic analysis and the method of characteristics and accounts for the coupling of incoming and outgoing characteristics. Furthermore in [7] it was shown in a test situation in which the flow would reach a steady state over a long time, the method proposed in [11] could lead to an incorrect steady state. The current study considers periodic flows. Moreover, all possible types and techniques of boundary conditions are included in this study. The technique recommended by [7] proved superior to all others considered, and matched the results of asymptotic methods which are valid for low subsonic Mach numbers.

*Supported in part by NSF Grant DMS-8921189, and by NASA cooperative agreement NCC-3-104.

1 Introduction

This paper deals with an exterior problem governed by compressible, inviscid gas dynamics equations. The nonlinear nature of the problem calls for a numerical solution to the problem. As common to most exterior problems, the condition(s) that must be satisfied at infinity is the key to solve these problems uniquely. The conditions that are physically correct are not necessarily mathematically correct for the well-posed-ness of the problem. Among the well known examples the one that stands out in the literature is the exterior problem governed by the Helmholtz equation. The class of problems that is governed by this equation include scattering of acoustic and electromagnetic waves. While physically, the quantities decay to zero at infinity, the requirement being exactly zero at infinity is not a well posed condition, as observed by Hellwig (see reference[10]). The same holds true for the Euler equations under consideration. Moreover, the computational considerations require that these problems are to be solved in a finite domain with the aid of an artificial boundary placed sufficiently far away from the region of local flows that are of interest. This introduces another parameter L (eg. the radius of the artificial boundary) and the requirement of boundary condition(s) that should be consistent with the true infinite domain problem. Several efforts have been made along these lines. Most efforts consider linearized flows (linearized about the state at infinity) to obtain such classes of boundary conditions (For example see [2] and [6]). Among the first nonlinear versions of the boundary conditions for gas dynamics problems was that of Hedstrom [9]. Recently Thompson [11] extended the ideas of Hedstrom to multidimensional problems. His procedure works well for two dimensional problems described in Cartesian coordinates with rectangular boundaries. Thompsons method works because in Cartesian coordinates the flux term of the equation for the outgoing wave can be neglected. Although this technique can be implemented in spherical and cylindrical coordinate systems, it will produce poor results because the equations for the outward and inward propagating wave variables are coupled in the flux term.

There is another parameter that is present in the computational model. This parameter is the total length of computational time, T. For problems that require long time stability, such as the ones considered in this paper, the ideas of [3] cannot be used as these are high frequency boundary conditions. They will be accurate for short times and one cannot expect them to work well for any long time calculations.

Motivated by the work of Hagstrom and Hariharan [7] and the asymptotic work of Geer and Pope [5] as well as Hardin and Pope [8], we model the external flow around a sphere pulsating in the air. This problem is of considerable interest from a mathematical standpoint as a testing ground for various versions of time dependant open boundary conditions and asymptotic methods. Until recently, such boundary conditions have all been linear, and based on non-reflection, however for many problems such as the pulsating sphere, or jet flow computations, the the nonlinearity is important, and the waves are coupled such that an outward propagating wave will generate an inward travelling wave. Exceptions to these kind of conditions are the technique of [7], which is a nonlinear reflective condition that is based on asymptotic analysis, and the nonlinear non reflective technique of Thompson [11]. This work applied the above methods to the case of fully unsteady flow resulting from a pulsating sphere. Furthermore various other boundary conditions were assessed along with the ones in [7] and [11].

2 Model and Derivation

Considering isentropic, compressible flow the Euler equations are given by

$$\frac{\partial \rho}{\partial t} + \nabla \cdot (\rho \vec{u}) = 0, \tag{1}$$

$$\nabla p + \rho(\frac{\partial \vec{u}}{\partial t} + (\vec{u} \cdot \nabla)\vec{u}) = 0, \tag{2}$$

$$p = k\rho^{\gamma}. \tag{3}$$

Equations (1) and (2) are known as the conservation of mass and momentum equations, and (3) is an isentropic constitutive law. Here ρ is density, $\vec{u}$ is the velocity field vector, p is pressure, t is time, and k and γ are constants characteristic to the medium. The model problem considered is the special case of a sphere harmonically pulsating in a fluid medium. Accordingly, the first assumption in this problem is that the flow is spherically symmetric and the governing equations take the form

$$\frac{\partial \rho}{\partial t} + \frac{\partial}{\partial r}(\rho u) = -\frac{2\rho u}{r}, \tag{4}$$

$$\frac{\partial}{\partial t}(\rho u) + \frac{\partial}{\partial r}\left(p + \rho u^2\right) = -\frac{2\rho u^2}{r}, \tag{5}$$

$$p = k\rho^{\gamma}. \tag{6}$$

Then we scale the variables in the following manner:

$$\rho = \rho_0 \hat{\rho}, \tag{7}$$

$$u = U\hat{u}, \tag{8}$$

$$r = L\hat{r}, \tag{9}$$

$$t = (L/C_0)\hat{t}, \tag{10}$$

where U, ρ_0, and L are a radial velocity, density, and length characteristic to the problem and the local speed of sound of the medium is defined by

$$c^2 = \frac{\partial p}{\partial \rho} = k\gamma\rho^{\gamma-1}, \tag{11}$$

$$c_0 = c(\rho_0), \tag{12}$$

with the Mach number given as $M = U/c_0$. This scaling along with letting $z = M\rho u$ and implementing (6) yield the following nondimensionalized system

$$\frac{\partial \rho}{\partial t} + \frac{\partial z}{\partial r} = \frac{-2z}{r}, \tag{13}$$

$$\frac{\partial z}{\partial t}+\frac{\partial}{\partial r}\left(\frac{\rho^{\gamma}}{\gamma}+\frac{z^{2}}{\rho}\right)=\frac{-2z^{2}}{r\rho}. \tag{14}$$

Desiring that the sphere pulsate from a radius of unity at time $t = 0$ the pulsation of frequency w is implemented as a boundary condition on it's surface,

$$u(1,t) = M sin(wt), \tag{15}$$

while keeping the surface of the sphere at $r = 1$ to simplify computational aspects of the problem. Density, which is not specified on the sphere's surface, will be recovered from the governing equations through the method of characteristics. In the far field the gas should be undisturbed, thus $\rho \to 1$, and $u \to 0$ as $r \to \infty$. Initially we want the flow at rest, which implies that the initial conditions are $\rho(r,0) = 1$ and $u(r,0) = 0$.

3 Asymptotic Analysis

It was shown in [7] that the Euler equations (13) and (14) can be cast in terms of Riemann variables, R and S, as follows:

$$\frac{\partial R}{\partial t} + \left(\frac{z}{\rho} + \rho^{\frac{\gamma-1}{2}}\right)\frac{\partial R}{\partial r} = -\frac{2z}{r}\rho^{\frac{\gamma-3}{2}}. \tag{16}$$

$$\frac{\partial S}{\partial t} + \left(\frac{z}{\rho} - \rho^{\frac{\gamma-1}{2}}\right)\frac{\partial S}{\partial r} = \frac{2z}{r}\rho^{\frac{\gamma-3}{2}}. \tag{17}$$

where

$$R = \frac{z}{\rho} + \frac{2\rho^{\frac{\gamma-1}{2}}}{\gamma-1}. \tag{18}$$

and

$$S = \frac{z}{\rho} - \frac{2\rho^{\frac{\gamma-1}{2}}}{\gamma-1}. \tag{19}$$

This form is essential to examine the structure of far field solutions. Recall that the boundary conditions of the pulsating sphere are: $u(1,t) = M sin(wt)$, and also $\rho \to 1$, and $u \to 0$ as $r \to \infty$. Unfortunately an infinite domain is impossible to model in a computational sense, thus artificial boundary conditions are demanded. One method is to approximate infinity by a very large number, say L, and prescribe $\rho(L,t) = 1$ and $u(L,t) = 0$. Although simple to implement, this approximately physically correct boundary condition is not recommended since the effect of the pulsation must never propagate all the way to L or the solution will become invalid since the state variables are still time dependant for any finite L. The preferred way of handling an infinite domain is to adopt an Eulerian framework and observe the flow as it passes through a fixed volume. There are several approaches to building such boundaries. The approach recommended in this discussion will stem from an asymptotic analysis of the Riemann variables and will closely mimic the technique of [7] which proposed that if R and S could be approximated on the boundary then a more accurate artificial boundary condition could be developed. Thus we expanded the wave variables radially.

$$R = R_0 + \frac{R_1(r,t)}{r} + \frac{R_2(r,t)}{r^2} + \cdots \tag{20}$$

$$S = S_0 + \frac{S_1(r,t)}{r} + \frac{S_2(r,t)}{r^2} + \cdots \quad , \quad r \to \infty \tag{21}$$

Using the fact that R, and S are given in terms of the fluid properties

$$R = \frac{z}{\rho} + G, \tag{22}$$

$$S = \frac{z}{\rho} - G, \tag{23}$$

the values of R_0, and S_0 come from direct application of the far field data.

$$R_0 = -S_0 = \frac{2}{\gamma - 1} \tag{24}$$

Then by substituting

$$\rho^{\frac{\gamma-1}{2}} = \left(\frac{\gamma - 1}{4}\right)(R - S), \tag{25}$$

and

$$\frac{z}{\rho} = \frac{R + S}{2}, \tag{26}$$

the wave variable equations assume the following form,

$$\frac{\partial R}{\partial t} + \left(\frac{R+S}{2} + (\frac{\gamma-1}{2})\frac{R-S}{2}\right)\frac{\partial R}{\partial r} = -\frac{\gamma-1}{2r}\left(R^2 - S^2\right), \tag{27}$$

$$\frac{\partial S}{\partial t} + \left(\frac{R+S}{2} - (\frac{\gamma-1}{2})\frac{R-S}{2}\right)\frac{\partial S}{\partial r} = +\frac{\gamma-1}{2r}\left(R^2 - S^2\right). \tag{28}$$

Applying the asymptotic expansions

$$\begin{array}{c} \frac{\partial}{\partial t}(R_1/r + R_2/r^2 + \cdots) + \\ + \left[\begin{array}{c} (R_1 + S_1)/2r + (R_2 + S_2)/2r^2 + \cdots \\ +(\gamma - 1)/2\,(R_0 + (R_1 - S_1)/2r + (R_2 + S_2)/2r^2 + \cdots) \end{array} \right] \frac{\partial}{\partial r}(R_1/r + \cdots) \\ = -\frac{\gamma-1}{2r}\left(2(R_0R_1 - S_0S_1)/r + (2R_0R_2 + R_1^2 - 2S_0S_2 - S_1^2)/r^2 + \cdots\right), \end{array} \tag{29}$$

and,

$$\begin{array}{c} \frac{\partial}{\partial t}(S_1/r + S_2/r^2 + \cdots) + \\ + \left[\begin{array}{c} (R_1 + S_1)/2r + (R_2 + S_2)/2r^2 + \cdots \\ (\gamma - 1)/2\,(R_0 + (R_1 - S_1)/2r + (R_2 + S_2)/2r^2 + \cdots) \end{array} \right] \frac{\partial}{\partial r}(S_1/r + \cdots) \\ = -\frac{\gamma-1}{2r}\left(2(R_0R_1 - S_0S_1)/r + (2R_0R_2 + R_1^2 - 2S_0S_2 - S_1^2)/r^2 + \cdots\right), \end{array} \tag{30}$$

we obtain the first order problem,

$$\frac{\partial R_1}{\partial t} + \left(\frac{R_1 + S_1}{2r} + \frac{\gamma-1}{2}\left(R_0 + \frac{R_1 + S_1}{2r}\right)\right)\frac{\partial R_1}{\partial r} = 0, \tag{31}$$

$$\frac{\partial S_1}{\partial t} + \left(\frac{R_1 + S_1}{2r} - \frac{\gamma-1}{2}\left(R_0 + \frac{R_1 + S_1}{2r}\right)\right)\frac{\partial S_1}{\partial r} = 0, \tag{32}$$

which fits the form of Riemann invariants, that is, along the proper characteristic curves, R_1 and S_1 are constants. Furthermore, since there should be no incoming waves at $t = 0$ then $S_1(r, t) = 0$. The characteristic curve for R_1 given by

$$\frac{dr}{dt} = 1 + \left(\frac{1}{2} + \frac{\gamma - 1}{4}\right)\frac{R_1}{r} \tag{33}$$

defines the slope of the paths through space-time on which R_1 is constant, so that R_1 can be written as a function of only one variable distinguishing which curve it came from, $H(\tau) = R_1(r, t(r, \tau))$. Thus

$$\int \frac{dr}{1 + \left(\frac{1}{2} + \frac{\gamma-1}{4}\right) H(\tau)/r} = \int dt. \tag{34}$$

Then requiring that $t = \tau$ when $r = L$,

$$r - L - \left(\frac{1}{2} + \frac{\gamma - 1}{4}\right) H(\tau) \log \left|\frac{\left(\frac{1}{2} + \frac{\gamma-1}{4}\right) H(\tau) + r}{\left(\frac{1}{2} + \frac{\gamma-1}{4}\right) H(\tau) + L}\right| = t - \tau. \tag{35}$$

Note that we have not yet calculated R_1 on the boundary. The proposed boundary condition actually follows manipulation of the S_2 equation.

$$\frac{\partial S_2}{\partial t} - \left(1 + \left(\frac{\frac{\gamma-1}{4} - \frac{1}{2}}{r}\right) R_1\right) \frac{\partial S_2}{\partial r} = R_1, \tag{36}$$

Writing this in in terms of the characteristic for R_1

$$\frac{\partial S_2}{\partial \tau}\frac{\partial \tau}{\partial t} - \left(1 + \frac{(\gamma - 3)}{4r} H(\tau)\right) \left[\frac{\partial S_2}{\partial \tau}\frac{\partial \tau}{\partial r} + \frac{\partial S_2}{\partial r}\right] = H(\tau) \tag{37}$$

$$\frac{\partial S_2}{\partial \tau}\left[\frac{\partial \tau}{\partial t} - \left(1 + \frac{(\gamma - 3)}{4r} H(\tau)\right) \frac{\partial \tau}{\partial r}\right] - \left(1 + \frac{(\gamma - 3)}{4r} H(\tau)\right) \frac{\partial S_2}{\partial r} = H(\tau). \tag{38}$$

But

$$\frac{\partial \tau}{\partial t} = 1 \tag{39}$$

and

$$\frac{\partial \tau}{\partial r} = 1 - \frac{(\gamma + 1) H(\tau)}{4r^2 + (\gamma - 3) H(\tau)} \tag{40}$$

so that

$$\frac{\partial S_2}{\partial \tau}\left[1-\left(1+\frac{(\gamma-3)}{4r}H(\tau)\right)\left(1-\frac{(\gamma+1)H(\tau)}{4r^2+(\gamma-3)H(\tau)}\right)\right] - \left(1+\frac{(\gamma-3)}{4r}H(\tau)\right)\frac{\partial S_2}{\partial r} = H(\tau). \tag{41}$$

Now let

$$1/N(\tau,r) = 1-\left(1+\frac{(\gamma-3)}{4r}H\right)\left(1-\frac{(\gamma+1)H}{4r^2+(\gamma-3)H(\tau)}\right) \tag{42}$$

and

$$D(\tau,r) = \left(1+\frac{(\gamma-3)}{4r}H(\tau)\right). \tag{43}$$

Equation (38) can then be rewritten as

$$\frac{\partial S_2}{\partial \tau} - N(\tau,r)D(\tau,r)\frac{\partial S_2}{\partial r} = N(\tau,r)H(\tau). \tag{44}$$

Now along $dr/d\tau = -N(\tau,r)D(\tau,r)$

$$\frac{dS_2(r,\tau)}{d\tau} = N(\tau,r)H(\tau). \tag{45}$$

Given the initial conditions $S_2 = 0$ for $\tau = 0$, S_2 at L is given by

$$S_2(L,\tau) = \int_0^\tau H(s)N(s,\xi(s;\tau,L))ds \tag{46}$$

where

$$\frac{d\xi}{ds} = -ND, \tag{47}$$

and

$$\xi(\tau;\tau,L) = L. \tag{48}$$

Hence upon differentiating with respect to τ

$$\frac{\partial S_2}{\partial \tau} = H(\tau)N(\tau,L) + \int_0^\tau H(s)\frac{\partial}{\partial \tau}N(s,\xi(s;\tau,L))ds \tag{49}$$

$$\frac{\partial S_2}{\partial \tau} = R_1(L,\tau)N(\tau,L) + \int_0^\tau H(s)\frac{\partial}{\partial \xi}N(s,\xi(s;\tau,L))\frac{\partial \xi}{\partial \tau}ds. \tag{50}$$

Then considering

$$\frac{\partial N(\tau,r)}{\partial r} = -\left[\frac{(\gamma+1)8rH(\tau)}{(4r^2+(\gamma-3)H(\tau))^2} + \frac{2(\gamma-1)(\gamma-3)H^2(\tau)}{(4r^2+(\gamma-3)H(\tau))^2} + \frac{\gamma-3}{4r^2}H(\tau)\right.$$
$$\left. - \frac{(\gamma+1)(\gamma-3)H^2(\tau)}{4r^2(4r^2+(\gamma-3)H(\tau))}\right] \tag{51}$$
$$\times\left(1-\left(1+\frac{(\gamma-3)}{4r}H\right)\left(1-\frac{(\gamma+1)H}{4r^2+(\gamma-3)H(\tau)}\right)\right)^{-2},$$

which implies that $\partial N/\partial\xi$ causes the integral in (50) to be of order $1/r$ and thus contributing to the terms S_3 and higher. Using $R = R_0 + \frac{1}{r}R_1$, and $S = S_0 + \frac{1}{r^2}S_2$ the boundary condition at $r = L$ becomes,

$$\left.\frac{\partial S}{\partial t}\right|_{r=L} = \frac{R(L,t) - \frac{2}{\gamma-1}}{2L}. \tag{52}$$

In terms of the primitive variables we have

$$= \frac{z/\rho + \frac{2}{\gamma-1}\left(\rho^{\frac{\gamma-1}{2}} - 1\right)}{2L} \tag{53}$$

Thus the physical significance of this is that in the far field there is no incoming wave, and that at any fixed distance L the correction will be given in terms of the outgoing wave.

4 Numerical Implementation

4.1 Numerical Scheme

We have only considered a relatively simple second order accurate Lax-Wendroff algorithm. Higher order schemes can be applied with care in handling shock waves that are present in the current problem. To begin with, the continuity and momentum equations have been presented in a weak conservation law form, $\mathbf{U}_t + \mathbf{F}_r = -\mathbf{W}$, where,

$$\mathbf{U} = \begin{pmatrix} \rho \\ z \end{pmatrix}, \tag{54}$$

$$\mathbf{F} = \begin{pmatrix} z \\ z^2/\rho + \rho^\gamma/\gamma \end{pmatrix}, \tag{55}$$

$$\mathbf{W} = \begin{pmatrix} 2z/r \\ 2z^2/(\rho r) \end{pmatrix}. \tag{56}$$

In this format any of several schemes discussed by G.A. Sod [12] can be implemented. The notational convention adopted for the purpose of discretization is that a function of space-time, $\mathbf{F}(r,t) = \mathbf{F}_i^n$, with radius discretized by i, and time by n. In keeping with [7], the two step Lax-Wendroff scheme was chosen for its smoothness, and simplicity. For programming purposes the $\mathbf{U}$ vector is written as

$$\mathbf{U}_i^n = \begin{pmatrix} \rho(r_i, t_n) \\ z(r_i, t_n) \end{pmatrix} \tag{57}$$

The half step time values of $\mathbf{U}$ are denoted by $\mathbf{V}_i^n$. The updated values of $\mathbf{U}_i^{n+1}$ can then be written right back on top of $\mathbf{U}_i^n$ to save memory. The first step is given by

$$\mathbf{V}_i^n = \tfrac{1}{2}\left(\mathbf{U}_i^n + \mathbf{U}_{i+1}^n\right) - \tfrac{\Delta t}{2\Delta r}\left(\mathbf{F}(\mathbf{U}_{i+1}^n) - \mathbf{F}(\mathbf{U}_i^n)\right) - \tfrac{\Delta t}{2}\mathbf{W}(\tfrac{1}{2}(\mathbf{U}_i^n + \mathbf{U}_{i+1}^n), r_{i+\frac{1}{2}}) \tag{58}$$
$$i = 1, \cdots, N$$

and the second step is,

$$\mathbf{U}_i^{n+1} = \mathbf{U}_i^n - \tfrac{\Delta t}{2\Delta r}\left(\mathbf{F}(\mathbf{V}_i^n) - \mathbf{F}(\mathbf{V}_{i-1}^n)\right) - \Delta t \mathbf{W}\left(\tfrac{1}{2}(\mathbf{V}_i^n - \mathbf{V}_{i-1}^n), r_i\right) \tag{59}$$
$$i = 2, \cdots, N.$$

The next step is to implement the flux corrective transport algorithm (FCT) of Fletcher [4] in order to analyze the data and remove any spurious oscillations generated by the presence of shock waves.

4.2 Initial and Boundary Conditions

Implementation of this scheme requires initial and boundary data. Initially $\mathrm{U}(1,i,1)=1$, and $\mathrm{U}(2,i,1)=0$. The boundary data will come from the boundary conditions chosen at $r=1$ and $r=L$ which are discretized as $i=0$ and $i=N+1$ respectively. We will discuss five different methods.

4.2.1 Method One

Method one is the physically approximate conditions taken from the ambient state in the far field.

$$\rho(L,t)=1$$

and

$$z(L,t)=0$$

4.2.2 Method Two

Method two is Thompson's technique [11], which is to neglect the flux term in the governing S equation. This means at $r=L$ we have

$$\frac{\partial S}{\partial t}=\frac{2z\rho^{\frac{\gamma-3}{2}}}{r}. \tag{60}$$

In discretized form it reads

$$S(U_{N+1}^{n+1})=S(U_{N+1}^{n})+S(U_{N}^{n})-S(U_{N}^{n+1})+2\Delta t z_{N+1}\rho_{N+1}{}^{\frac{\gamma-3}{2}}/L. \tag{61}$$

Then use a discretized version of (71) to update R.

4.2.3 Method Three

Method three totally suppresses the incoming wave variable, that is set

$$\frac{\partial S}{\partial t}=0. \tag{62}$$

Discretized for the nonlinear case, update S as

$$S(U_{N+1}^{n+1})=S(U_{N+1}^{n})+S(U_{N}^{n})-S(U_{N}^{n+1}) \tag{63}$$

then, as in method two, use (71) to update R.

4.2.4 Method Four

Method four is the linearized version of method three, that is take

$$R = \frac{2}{\gamma - 1} + (\rho - 1) + z, \tag{64}$$

$$S = -\frac{2}{\gamma - 1} - (\rho - 1) + z, \tag{65}$$

and then apply

$$\frac{\partial S}{\partial t} = 0, \tag{66}$$

and equation (71) to update R and S.

4.2.5 Method Five

The boundary condition which we will show to have the best results is the one proposed in [7].

$$\left.\frac{\partial S}{\partial t}\right|_{r=L} = \frac{R(L,t) - \frac{2}{\gamma-1}}{2L} \tag{67}$$

where L is the truncation radius. Use of this boundary condition calls for an updated value of R. This means that not only (67) must be discretized, but also the partial differential equation for R. Writing (67) in the form

$$\frac{\partial S}{\partial t} = Q(\rho, z) \tag{68}$$

A simple second order discretization is,

$$S(U_{N+1}^{n+1}) = S(U_{N+1}^{n}) + S(U_N^n) - S(U_N^{n+1}) + 2\Delta t Q(V_N^n) \tag{69}$$

where $i = N + 1$ corresponds to $r = L$. Next the R equation in the form

$$\frac{\partial R}{\partial t} + C(\rho, z)\frac{\partial R}{\partial r} = H(\rho, z) \tag{70}$$

is discretized to,

$$\begin{gathered} R(U_{N+1}^{n+1}) = \\ \left(1/(1 + \tfrac{\Delta t}{\Delta r}C(V_N^n)\right) \Big[R(U_{N+1}^n) + R(U_N^n) \\ -R(U_N^{n+1}) + 2\Delta t H(V_i^n) \\ -\tfrac{\Delta t}{\Delta r}C(V_N^n)\left(R(U_{N+1}^n) - R(U_N^n) - R(U_N^{n+1})\right)\Big]. \end{gathered} \tag{71}$$

Then the primitive variables can be updated at the boundary using the updated boundary values of R and S with

$$\rho = \left(\frac{\gamma-1}{4}(R-S)\right)^{\frac{2}{\gamma-1}}, \tag{72}$$

$$z = \frac{1}{2}(R+S)\,\rho. \tag{73}$$

5 Results and Comparisons

As mentioned earlier, the governing equations were discretized using the two step Lax-Wendroff scheme. All numerical tests were conducted with the surface of the sphere pulsating with radial velocity $u = M sin(wt)$ where $w = 1.5$, and the Mach number set at, $M = 0.5$. The tests were designed to produce radial density and momentum profiles at time value $t = 10$. Initially we ran tests using a computational domain that was larger than the radius of propagation. This guaranteed that we had a solution that was independent of any boundary conditions. With a Mach number of $M = 0.5$ Gibbs phenomena became visible near the shock waves, displaying highly oscillatory behavior. A flux corrective transport subroutine by Fletcher [4] was employed to help capture the shocks and minimize oscillations as they occurred. To reassure the validity of the numerical solution it was necessary to compare it with a completely independent method. Asymptotics are often considered as alternatives to numerical solutions. Asymptotic solutions use the Mach as a parameter of expansion, thus requiring very low Mach numbers. The multiple scales technique of Geer and Pope [5] was chosen to compare with method one. Their first order approximation for velocity is given as

$$u_0(r,t) = \frac{(r-1)w}{(1+w^2)r^2}\cos(\tau) + \frac{1}{(1+w^2)}\left(w^2/r + 1/r^2\right)\sin(\tau) \tag{74}$$

and the second order correction is given as

$$\begin{aligned} u_1(r,t) &= (b_2/r^2 + 2b_3w/r)\cos(2\tau) + (b_3/r^2 - 2b_2w/r)\sin(2\tau) \\ &+ \left(\frac{(29-3\gamma)w^2}{16r^3(1+w^2)^2} + \frac{w^2(w^2-1)}{r^2(1+w^2)^2}\right)\cos(2\tau) - \frac{(1+\gamma)w^2\log(r)}{4r^2(1+w^2)} \\ &+ \left(\frac{(29-3\gamma)w(w^2-1)}{32r^3(1+w^2)^2} - \frac{2w^3}{r^2(1+w^2)^2}\right)\sin(2\tau) \end{aligned} \tag{75}$$

where

$$f(t) = (\sin(wt) - w\cos(wt)/\left(1+w^2\right) \tag{76}$$

$$r^2 = \eta^2 + (\gamma+1)M(r-1)f'(t+1-\eta) \tag{77}$$

$$\tau = w(t+1-\eta) \tag{78}$$

and

$$b_2 = -\frac{3w^2(14 - 2\gamma + 17w^2 + \gamma w^2)}{16(1+w^2)^2(1+4w^2)} \tag{79}$$

$$b_3 = \frac{w(29 - 3\gamma - 17w^2 + 15\gamma w^2 - 64w^4)}{32(1+w^2)^2(1+4w^2)}. \tag{80}$$

Then the velocity is calculated as

$$u(r,t) = u_0(r,t) + Mu_1(r,t). \tag{81}$$

Figure 1 shows a velocity profile of [5] compared with the numerical method at time, $t = 10$, generated with Mach number, $M = 0.05$. These solutions agree fairly closely.

If an artificial boundary was placed at a radius where waves would pass through it by time $t = 10$ then the effect of the artificial boundary conditions could be evaluated by comparing it to the profiles calculated in a large domain which was independent of boundary conditions. A perfect boundary condition would yield a profile that perfectly matched these examples regardless of where the radius was truncated. In figure 2 the physically approximate boundary conditions of method one were evaluated at $r = 6$, $r = 7$, and $r = 9$. Figure 2 clearly shows that this physical approximation is invalid for truncations inside of the radius of propagation.

In figure 3 Thompsons method [11], method two, has been run at three different truncation radii, $L = 21$ ($L = 21$ corresponds to 2000 nodes.), $L = 7$, and $L = 3$. If the method two boundary condition was numerically correct, the profiles for $L = 7$, and $L = 3$ should virtually coincide with the profile for $L = 21$. Thompson's boundary condition has caused the numerical scheme to undershoot the $L = 21$ profile when truncated at $L = 3$, this is because Thompsons boundary condition will go to zero in the far field independent of the behavior of the density.

The results of method three, the nonlinear suppression of the incoming wave, also truncated at $L = 21$, $L = 7$, and $L = 3$, are given in figure 4. The basic difficulty is the fact that even though this method was based on the Riemann variables, it did not simulate the movement of the waves because it did not exploit the governing equations of the Riemann variables (16) and (17).

Figure 5 presents the results of method four, the linearized suppression of the incoming wave, when truncated at $L = 21$, $L = 7$, and $L = 3$ as in the previous tests. Although not perfect, this technique does not perform badly for ten time units. The amplitude of overshoot from the $L = 3$ truncation indicates that this method will not stay stable in a far time application. Thus as time is increased the profile would continue to deviate.

The results of the technique proposed in [7], method five, as shown in figures 6, 7, and 8, are far superior to the other four methods which offer no hope for solutions in long time calculations . In figure 6 the profiles generated with truncations at $L = 3$ and $L = 7$ lay precisely on the profile of truncation at $L = 21$. This same style test was then performed on method five at time $t = 100$ and $t = 1000$ (one million time steps) to see if it would remain stable for a far time situation. In figures 7 and 8 the truncated profiles continue to coincide, indicating that this technique precisely simulates waves passing the artificial boundary and is dependable regardless of the time value to which the scheme is run.

It is useful to examine the nature of the solutions as $w \to 0$ and as $w \to \infty$. As one would expect, the variation of the solution in the computational domain are small for low frequencies. Figure 9 shows this for decreasing values of w using method five. (In this case the nonlinear effects are more prominent in the far field than in the near field.) On the other hand for high frequency waves an increase in the frequency reflects more periodic structures of the shock waves. Figure 10 shows a tenfold increase in the number of shock fronts by going from $w = 1.5$ to $w = 15$. However further increase in the frequency poses a challenge for the numerical computations. As the frequency increases the fronts are closer to each other. In the extreme cases one must develop an asymptotic solution to these problems. For example figure 10 suggests that the solution rapidly attenuates for $w = 150$. These asymptotic aspects require further study.

Considering figure 9, method five works quite well for low frequency problems, but this was not the case for all other classes of boundary conditions. In figure 11 we show the solution of Thompson for $w = .015$, with $L = 11$ and $t = 100$. For $t = 100$ the sphere will not have gone through a full oscillation, but the wave will have passed our truncation point at $L = 11$. This solution approaches an incorrect state well below what would be expected (compare with figure 9), Thus it is not uniformly accurate in time. The method proposed in [7] is indeed a uniformly valid condition due to its derivation that is based on uniform asymptotic expansions.

6 Conclusion

This paper has modeled the flow field generated by a pulsating sphere. This modeling process involved exploring the laws of gas dynamics and combining these laws with mathematical analysis in order to obtain numerical solutions for the flow field. Because of the intrinsic spherical symmetry of the problem the solutions naturally took the form of radial density and velocity profiles for specified times of interest. The numerical implementation of the governing equations was of particular mathematical interest because it became necessary to include a flux corrective transport algorithm to help control the numerical instabilities generated by the presence of shock waves.

The next topic to be addressed in the modeling process was to come up with suitable numerical boundary conditions. Following the lead of Hagstrom and Hariharan [7] a method of characteristics representation was created to sense the presence of incoming and outgoing waves, and then implemented as a numerical boundary condition. The boundary condition was then evaluated along with several other techniques for stability far in time, and consistency regardless of the radius at which the domain was truncated. This discussion revealed that for the numerical solution of problems in gas dynamics the modeling of the open boundary conditions is critical. The wrong form of these conditions, especially in fully unsteady flow, can lead to a completely incorrect solution. Yet from all this, the technique of [7] has proven to be a dependable method for problems that can be modeled as having spherical wavefronts in the far field. Future work in this field is the generalized boundary condition for fully three dimensional unsteady flow.

References

[1] M.B. Abbot, *An Introduction To The Method of Characteristics*, Thames and Hudson, 1966.

[2] A. Bayliss, E. Turkel, *Far field boundary conditions for compressible flows*, J. Comp. Phys., 1982, 48, 182-199.

[3] B. Enquist, A. Majda, *Absorbing boundary conditions for the numerical simulation of waves*, Math. Comp., 1977, 31, 629-651.

[4] C.A.J. Fletcher, *Computational Techniques for Fluid Dynamics*, Vol. II, Springer-Verlag, 1988

[5] J. Geer, D. Pope, *A Multiple Scales Approach to Sound Generation by Vibrating Bodies*, ICASE Report No. 92-73, 1992.

[6] B. Gustafsson, *Far field boundary conditions for time dependant hyperbolic systems*, SIAM J. Sci. Stat. Comp., 1988, 9, 812-828.

[7] T. Hagstrom, S.I. Hariharan, *Accurate Boundary Conditions for Exterior Problems in Gas Dynamics*, Mathematics of Computation, Vol.51,No.184, Oct. 1988.

[8] J.C. Hardin, D.S. Pope, *A New Technique for Aerodynamic Noise Calculation*, DGLR/AIAA 92-02-076.

[9] G. W. Hedstrom, J. Comp. Phys., 1979, 30,222

[10] G. Hellwig, *Partial differential equations*, Blaisdell, Waltham, Mass., 1964.

[11] K. Thompson, *Time Dependant Boundary Conditions for Hyperbolic Systems*, Journal of Computational Physics, Vol.68, No.1, 1987.

[12] G. Sod, *A Survey of Several Finite Difference Methods for Systems of Nonlinear Hyperbolic Conservation Laws*, Journal of Computational Physics 27, 1-31 (1978).

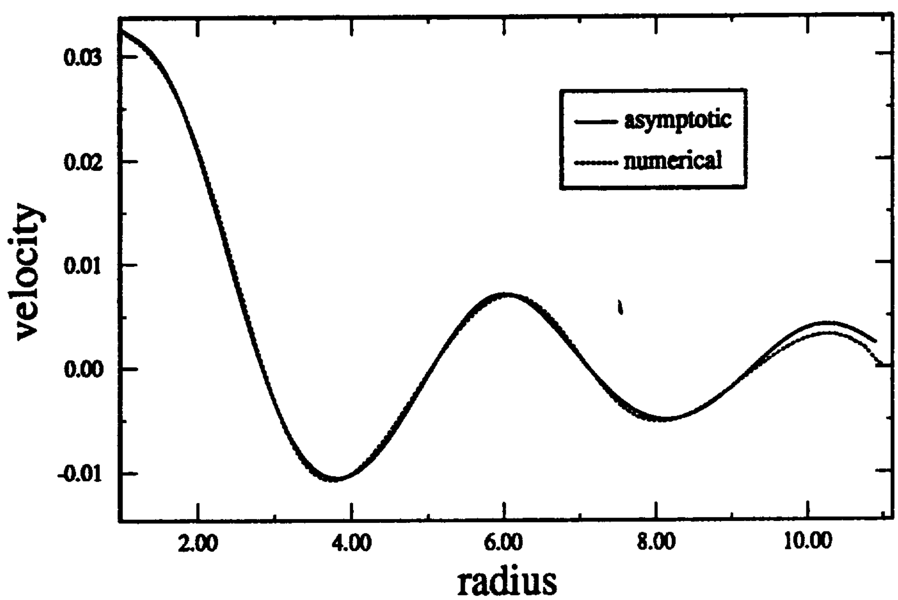

Figure 1: Asymptotic technique vs. Numerical method for Mach number $M = 0.05$

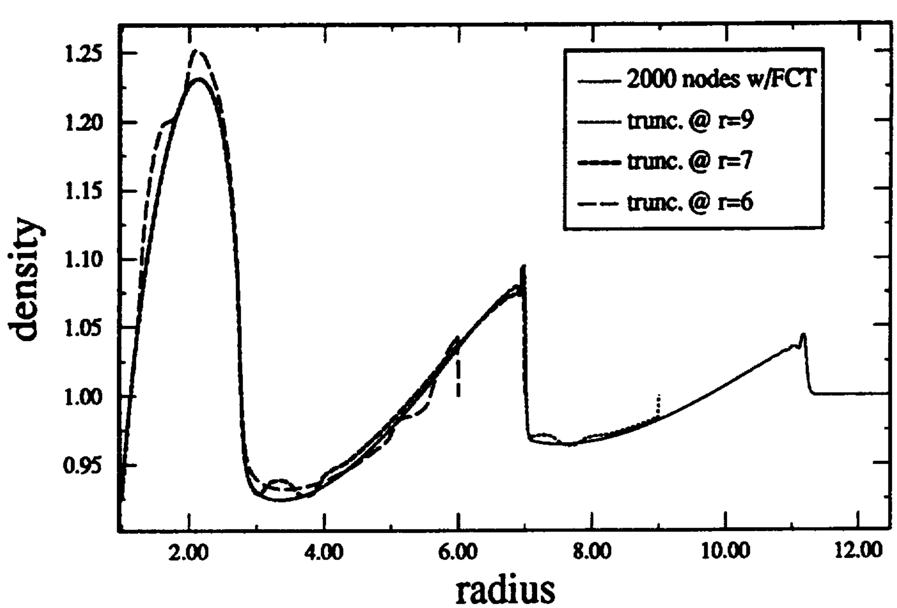

Figure 2: Physically approximate boundary conditions

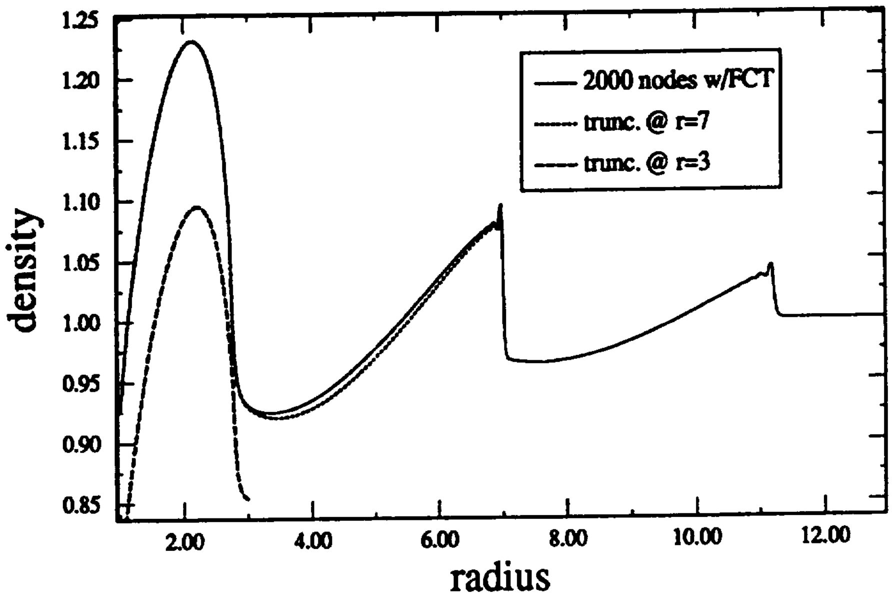

Figure 3: The boundary condition of Thompson

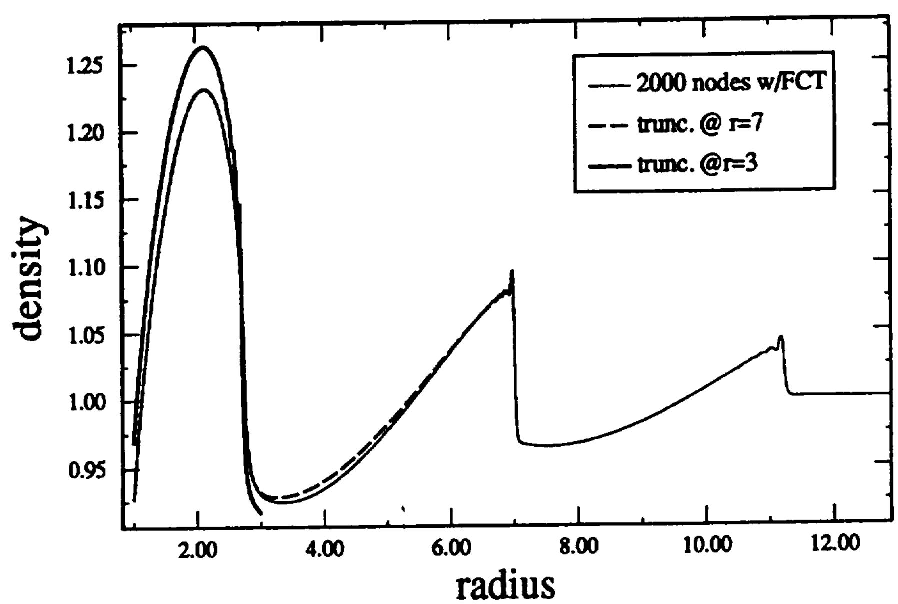

Figure 4: Nonlinear suppression of the incoming wave

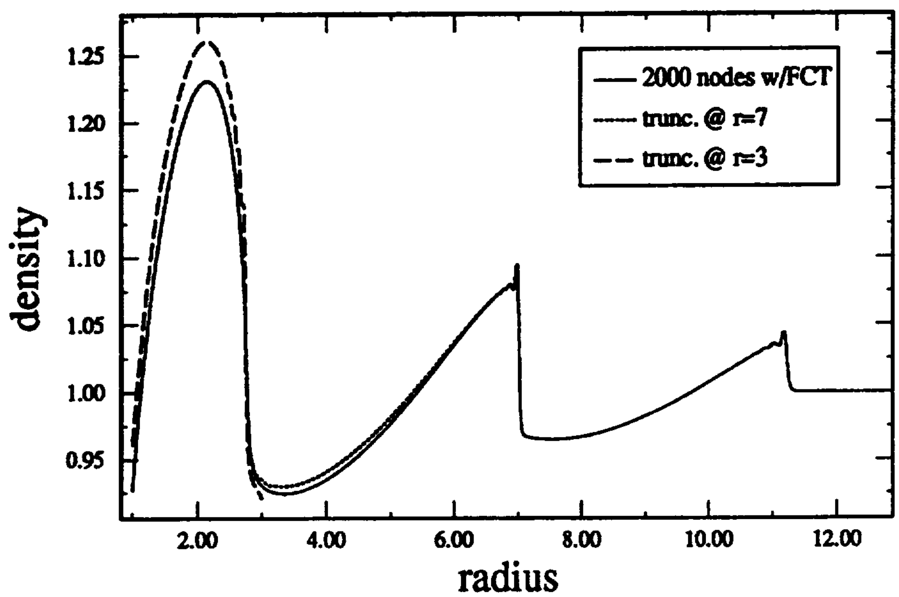

Figure 5: Linearized suppression of the incoming wave

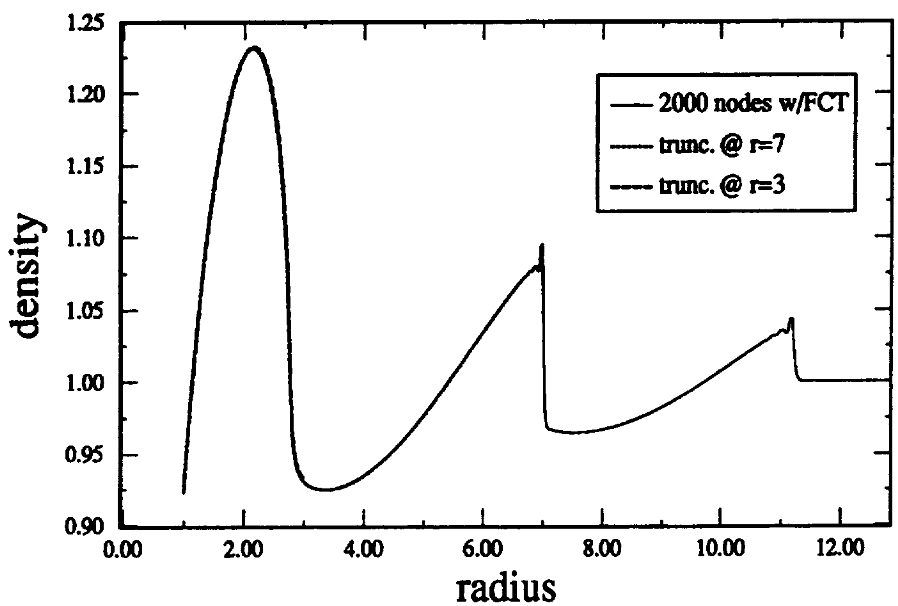

Figure 6: The method of Hagstrom and Hariharan

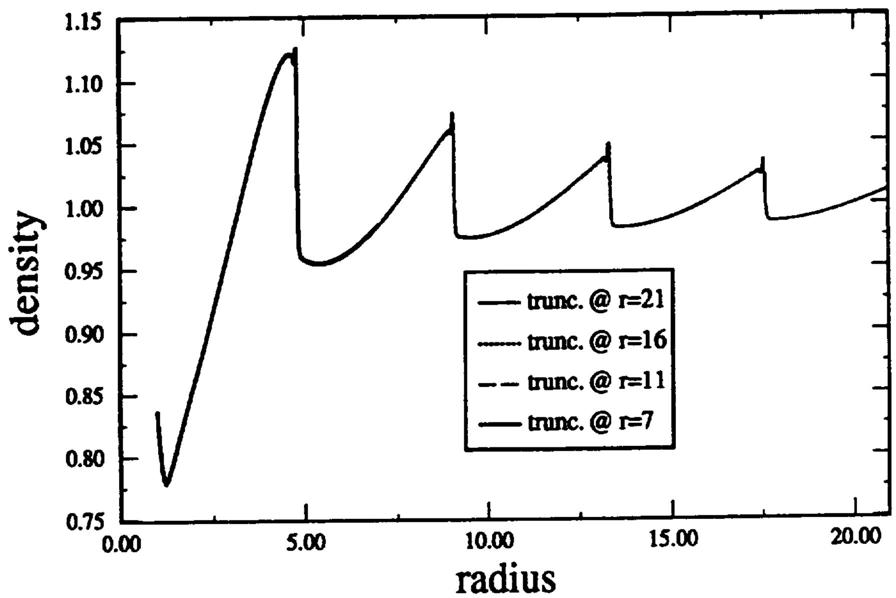

Figure 7: The method of Hagstrom and Hariharan at $t = 100$

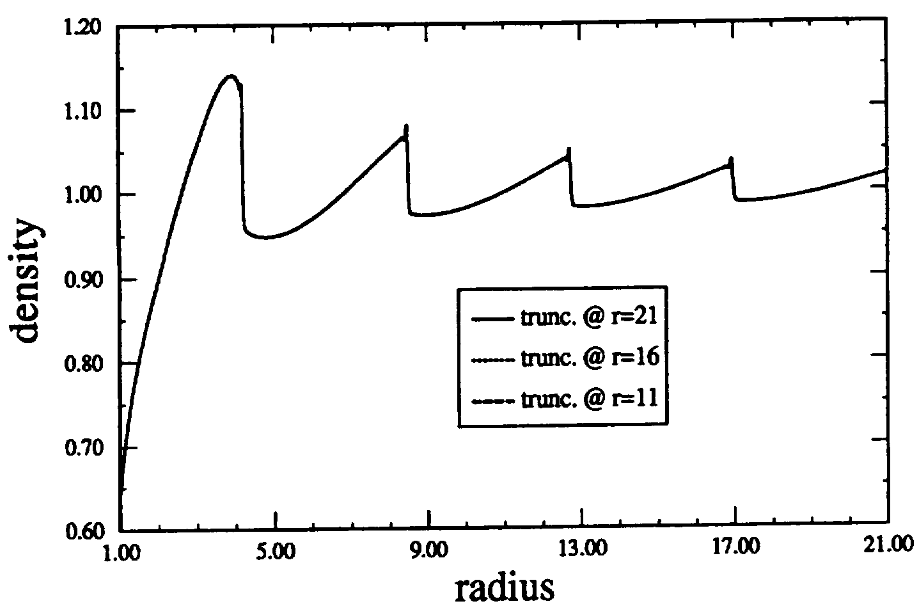

Figure 8: The method of Hagstrom and Hariharan at $t = 1000$

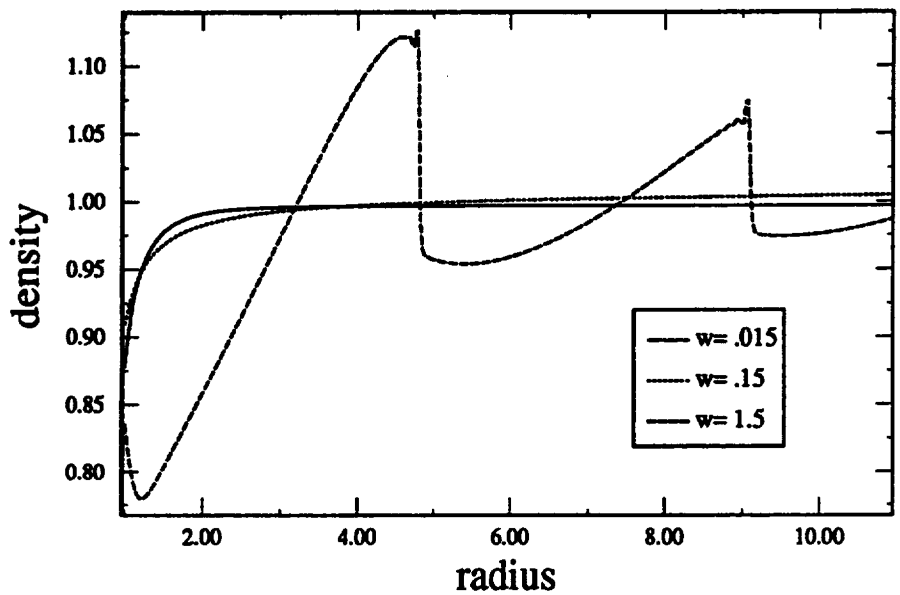

Figure 9: Density profiles from low frequency pulsation, t=100

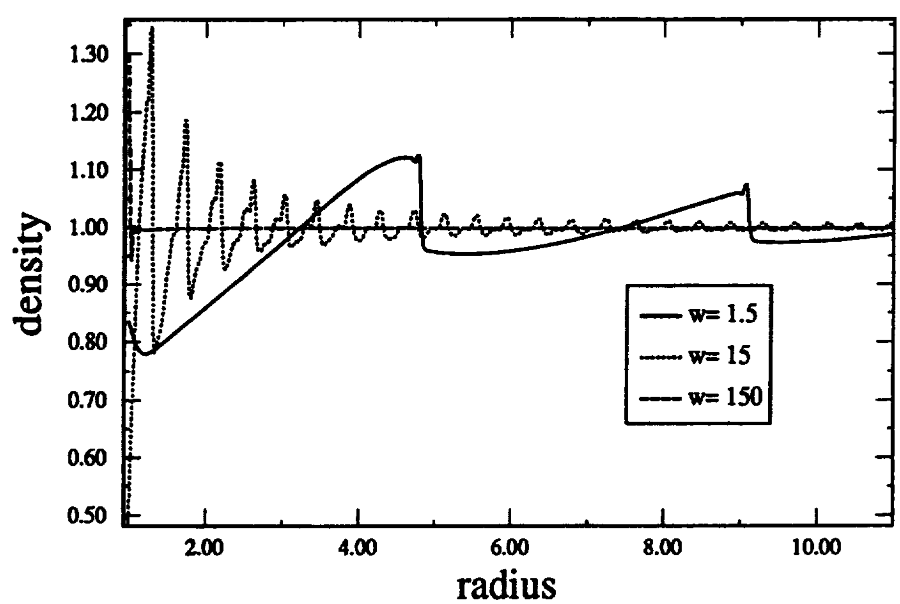

Figure 10: Density profiles from high frequency pulsation, t=100

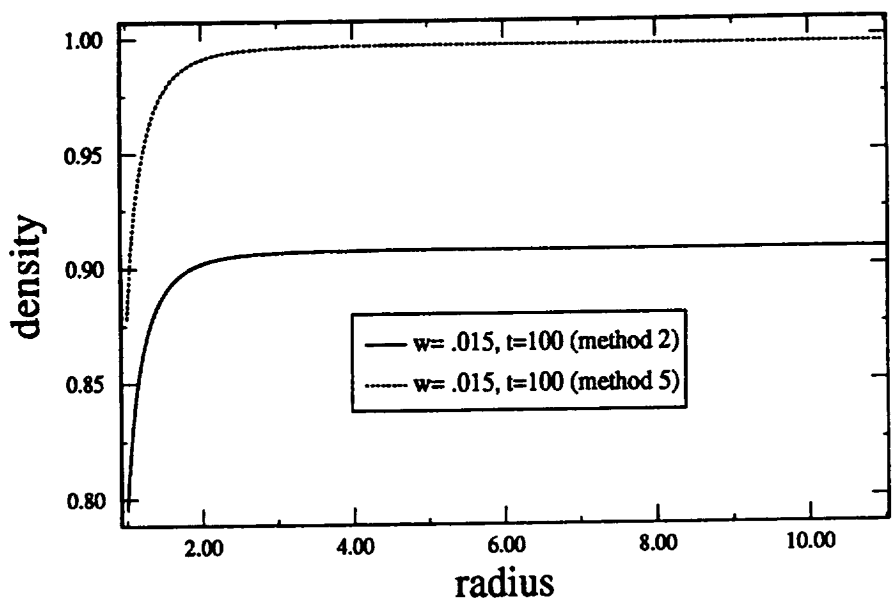

Figure 11: Density profiles for w=.015, r=11, and t=100

REPORT DOCUMENTATION PAGE

Form Approved
OMB No. 0704-0188

1. AGENCY USE ONLY (*Leave blank*)	2. REPORT DATE	3. REPORT TYPE AND DATES COVERED
	September 1994	Technical Memorandum

4. TITLE AND SUBTITLE

Boundary Conditions for Unsteady Compressible Flows

5. FUNDING NUMBERS

WU-505-90-5K

6. AUTHOR(S)

S.I. Hariharan and D.K. Johnson

7. PERFORMING ORGANIZATION NAME(S) AND ADDRESS(ES)

National Aeronautics and Space Administration
Lewis Research Center
Cleveland, Ohio 44135-3191

8. PERFORMING ORGANIZATION REPORT NUMBER

E-9138

9. SPONSORING/MONITORING AGENCY NAME(S) AND ADDRESS(ES)

National Aeronautics and Space Administration
Washington, D.C. 20546-0001

10. SPONSORING/MONITORING AGENCY REPORT NUMBER

NASA TM-106737
ICOMP-94-22

11. SUPPLEMENTARY NOTES

S.I. Hariharan, Institute for Computational Mechanics in Propulsion, NASA Lewis Research Center, (work funded under NASA Cooperative Agreement NCC3-233 and supported in part by NSF Grant DMS-8921189 and NASA Cooperative Agreement NCC3-104), and the University of Akron, Akron, Ohio 44325; D. K. Johnson, the University of Akron, Akron, Ohio 44325. ICOMP Program Director, Louis A. Povinelli, organization code 2600, (216) 433-5818.

12a. DISTRIBUTION/AVAILABILITY STATEMENT

Unclassified - Unlimited
Subject Category 34

12b. DISTRIBUTION CODE

13. ABSTRACT *(Maximum 200 words)*

This paper explores solutions to the spherically symmetric Euler equations. Motivated by the work of Hagstrom and Hariharan and Geer and Pope, we modeled the effect of a pulsating sphere in a compressible medium. The literature available on this suggests that an accurate numerical solution requires artificial boundary conditions which simulate the propagation of nonlinear waves in open domains. Until recently, the boundary conditions available were in general linear and based on nonreflection. Exceptions to this are the nonlinear nonreflective conditions of Thompson, and the nonlinear reflective conditions of Hagstrom and Hariharan. The former are based on the rate of change of the incoming characteristics; the latter rely on asymptotic analysis and the method of characteristics and account for the coupling of incoming and outgoing characteristics. Furthermore, Hagstrom and Hariharan have shown that, in a test situation in which the flow would reach a steady state over a long time, Thompson's method could lead to an incorrect steady state. The current study considers periodic flows and includes all possible types and techniques of boundary conditions. The technique recommended by Hagstrom and Hariharan proved superior to all others considered and matched the results of asymptotic methods that are valid for low subsonic Mach numbers.

14. SUBJECT TERMS

Unsteady flow; Boundary conditions

15. NUMBER OF PAGES

27

16. PRICE CODE

A03

17. SECURITY CLASSIFICATION OF REPORT	18. SECURITY CLASSIFICATION OF THIS PAGE	19. SECURITY CLASSIFICATION OF ABSTRACT	20. LIMITATION OF ABSTRACT
Unclassified	Unclassified	Unclassified	